Magnesium Technology 2011
Edited by: Wim H. Sillekens, Sean R. Agnew, Neale R. Neelameggham, and Suveen N. Mathaudhu
TMS (The Minerals, Metals & Materials Society), 2011

IN-SITU SCANNING ELECTRON MICROSCOPY COMPARISON OF MICROSTRUCTURE AND DEFORMATION BETWEEN WE43-F AND WE43-T5 MAGNESIUM ALLOYS

Tomoko Sano[1], Jian Yu[1], Bruce Davis[2], Richard DeLorme[2], Kyu Cho[1]
1. US. Army Research Laboratory, Materials and Manufacturing Science Division, Aberdeen Proving Ground, MD 21005 USA
2. Magnesium Elektron North America, 1001 College St. Madison, IL 62060 USA

Keywords: In-situ, magnesium, microstructure, deformation

Abstract

In-situ tensile testing in the scanning electron microscope was used to investigate the quasi-static deformation behavior and fracture mechanism of WE43 magnesium alloys. The in-situ tensile experiments were conducted at room temperature at a constant crosshead speed of 0.5 mm / min. One set of samples was a rolled and quenched F temper alloy and the other set was an artificially aged T5 temper alloy. The objective of this research was to determine the effect of tempering on precipitates chemistries, microstructure, and mechanical properties. The sample orientation is known to affect the tensile properties. Hence tensile specimens with different sample orientation were tested. The crystallographic orientations were characterized by electron backscattered diffraction. Strong textures were observed with rolling plane crystals indicating a basal plane orientation.

Introduction

Magnesium Elektron's Elektron™ WE43, developed initially as a sand casting alloy, was found to have good mechanical properties, creep and corrosion resistance, and good strength retention after exposure to elevated temperatures[1]. Elektron™ WE43 has the nominal wt% composition of Mg-(3.7 – 4.3)Y- (2.0-2.5)Nd-(0.4-2.4) Heavy Rare Earth elements-(0.4)Zr. Because of its castability, and creep and corrosion resistances, it is well known that there is interest by the aerospace and automotive industries. Due to Mg's low density[2], the Army is also interested in Mg alloys for numerous lightweight structural and engineered material applications.

There have been some recent research in the area of casting and process control of WE43, using computer simulations to determine the best casting parameters and optimizing the processsing[3]. This paper explores further into the processing, but at the mesoscale for optimization of the microstructure. The objective of this research is to understand the strengthening effects based on the homogenization and the T5 tempering process. Homogenization, which is a heat treatment at a temperature ranging from 200 to 600 °C for several hours, affects the precipitate formation. Some precipitates have been observed to affect hardness[4] and improve mechanical properties[5, 6] by Y additions[7] and by dispersion strengthening[8]. The objective is to characterize the precipitates chemistries, microstructure, and mechanical properties of the as-rolled WE43 –F and homogenized and artificially aged WE43-T5 tempered alloys. In this paper, current results identifying the effects of T5 heat treatments on the quasistatic tensile response of Elektron™ WE43 is discussed.

Experimental Procedures

Elektron™ WE43 -F and WE43 -T5 tensile specimens with a gauge length of 15 mm, width of 3 mm, and thickness of 1 mm (see Fig. 1) were milled in the longitudinal direction and transverse directions from rolled plates. The samples were mechanically polished starting with 600 grit SiC disc coated with wax, then with glycol based diamond solution of incrementally decreasing particle size on polishing cloth until reaching the 0.25 micron particle size. Further polishing with 0.04 micron colloidal silica on final polishing cloth was performed for samples to be examined by the scanning electron microscope (SEM), energy dispersive spectroscopy (EDS), and electron backscattered diffraction (EBSD).

The FEI Nova NanoSEM 600 SEM was used to characterize the microstructure before and after the tensile tests. EDS (EDAX Genesis) was used to determine the precipitate chemistry for both F and T5 samples. EBSD characterization of the crystallographic orientation texturing of the F and T5 samples were conducted at 20 kV accelerating voltage, spot size of 5, and at 70° tilt with the EDAX/TSL EBSD system in the SEM. EBSD patterns were collected from surfaces perpendicular to the rolling direction, normal direction, and the transverse direction for both WE43 samples. The collected data was minimally "cleaned" with the TSL OIM Analysis 5 "cleanup" program to correct incorrectly indexed points based on neighboring point's orientation correlation.

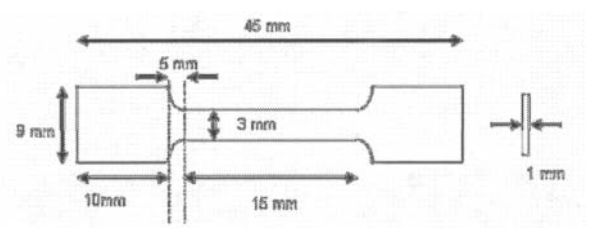

Figure 1. Tensile specimen geometry

The Ernest Fullam in-situ tension and compression stage for the SEM (see Fig. 2) coupled with the ADMET's MTEST Quattro™ interface and application program was used for the tension experiments. Strain rates on the order of 10^{-4} s^{-1} were applied for all samples. To determine a more accurate Young's modulus, digital image correction (DIC) technique was applied. During the tensile test, in the elastic regime, a series of SEM images of the microstructure were captured and corresponding live loads and positions were recorded. The image size was 1024 × 943 pixels; the field of view was about 4 × 4 mm^2. Then, the TIFF images were imported into GOM mbH's ARAMIS, a photogrammetric software, for strain analysis. The analysis

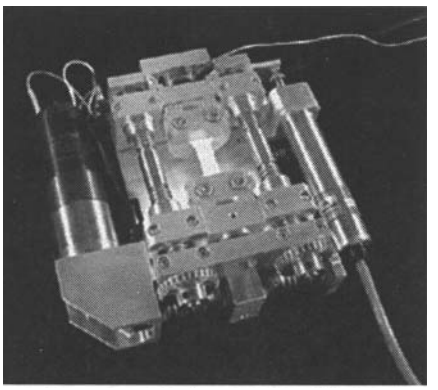

Figure 2. Ernest Fullam in-situ tension-compression stage

procedure for ARAMIS was detailed in earlier report[9]. Here, we used the 2-dimensional analysis procedure, in which only one camera view was required. The optimal facet size is 51 × 51 pixels and the optimal facet step overlap is 25 pixels. A signal filter was applied to remove noise (2 × 7 filter runs; replacing the facet point value with the median value among the 49 neighboring facet points and itself). In addition to the local strain contour plots, three virtual digital strain gauges were placed on the specimen surface to obtain the average bulk strain. The average bulk strain and load values were used to plot more accurate stress strain curves to calculate the Young's modulus.

Results

When examined under the SEM, the microstructures of both the F and T5 tempers revealed obvious precipitation, as shown in Fig 3. Precipitates are known to contribute to the strengthening of WE43 alloys[4, 10]. The finer precipitates are most likely attributed to the metastable β", β', intermediate β_1, and stable β phases[4, 10, 11]. Analysis of those and other precipitates are currently being conducted with a transmission electron microscope for this research. The larger rectangular precipitates and the oval shaped precipitates are believed to be $Mg_{24}Y_5$, and $Mg_{41}Nd_5$, respectively[12, 13]. EDS analysis of these larger precipitates showed that the oval precipitates were Nd-rich and the rectangular precipitates were Y-rich (see Fig. 4 and 5).

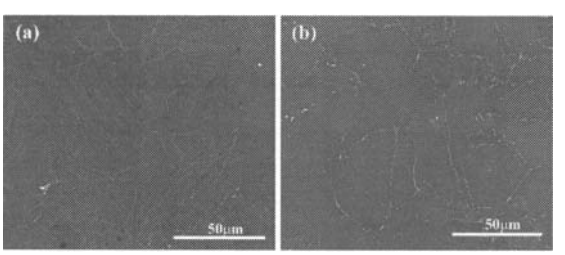

Figure 3. SEM image of the plate surface of (a) WE43 –F and (b) WE43 –T5.

From the in-situ micro tensile experiments, load over elongation data were obtained and engineering stress – strain curves were plotted, as shown in figure 6. DIC technique was used to collect data and plot the stress – strain curves in the elastic regime. By comparison of the moduli calculated from the stress – strain curves from the ADMET data to those calculated from DIC data, it was determined that the DIC data was more accurate along

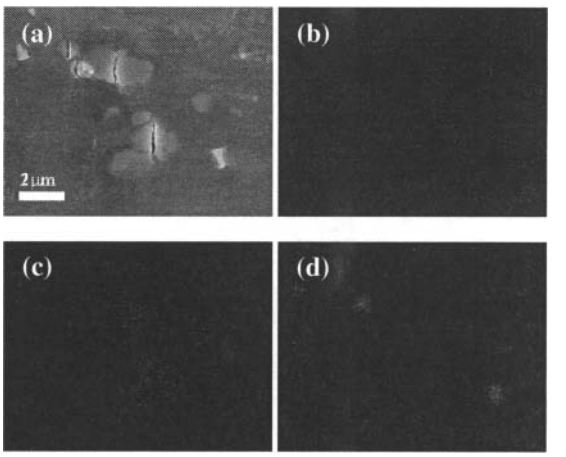

Figure 4. (a) Secondary electron image of the mapped area of WE43 -F. (b) Blue points indicating the presence of Mg, (c) Nd in purple and (d) Y in yellow.

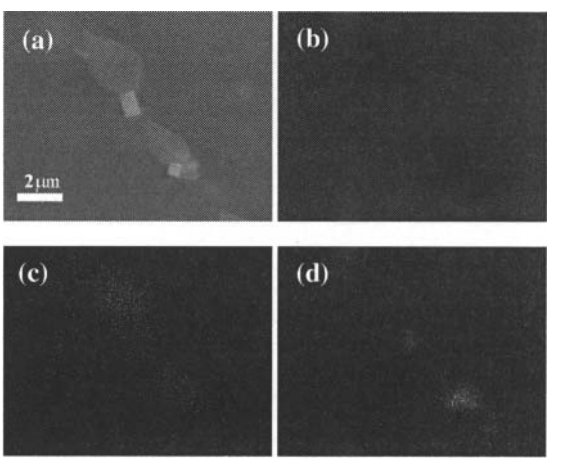

Figure 5. (a) Secondary electron image of the mapped area of WE43 –T5. (b) Blue points indicating the presence of Mg, (c) Nd in purple and (d) Y in yellow.

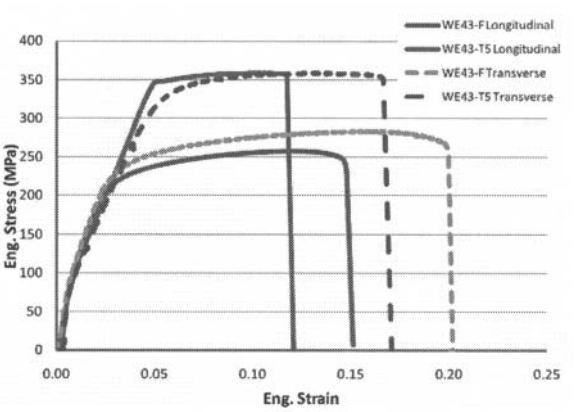

Figure 6. Example stress – strain curves of the –F and –T5 samples in the longitudinal and transverse directions.

the elastic regime. The average ultimate tensile stresses from the ADMET data, elongations, and moduli from the DIC data are tabulated in Table I. Post mortem analyses of the fracture surfaces were conducted. Though both F and T5 samples in both longitudinal and transverse directions failed by microvoid coalescence, the T5 sample showed the influence of less ductility (see Fig 7). In addition, there is evidence of a more brittle rupture mechanism in play for the T5 samples.

TABLE I. UTS, Elongation, and Young's Modulus for the F and T5 samples

Sample	UTS (MPa)	% Elongation	Young's Modulus (GPa)
WE43–F Longitudinal	273.2	20.5	25.0
WE43–F Transverse	283.2	20.0	34.5
WE43–T5 Longitudinal	331.7	10.5	25.8
WE43–T5 Transverse	358.6	13.3	34.1

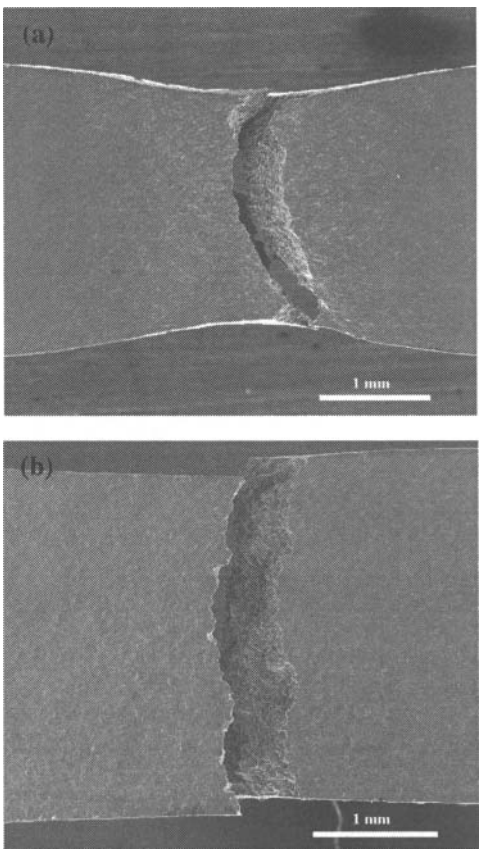

Figure 7. Failure region of (a) an F sample and (b) T5 sample.

Texturing of the surfaces was observed for both –F and –T5 samples from the collected EBSD patterns. The basal plane orientation was the most observed orientation in the surface parallel to the plate, while the plane orientations in the surfaces perpendicular to the rolling direction and transverse direction tended to be prismatic planes. This is in agreement with observations reported by Senn and Agnew[14]. Figure 8 shows a schematic of the orientations in the corresponding surfaces of the T5 plate. The schematic's surfaces are made up of one set of EBSD inverse pole figure maps from EBSD patterns obtained from each of the plate surfaces. The F tempered samples also showed similar texturing of the surfaces in relation to the plate's rolling and transverse directions. To better compare the differences between the F and T5, or the effect of the homogenization and aging on the orientation distribution, inverse pole figures of the surface orientations were plotted in Fig. 9.

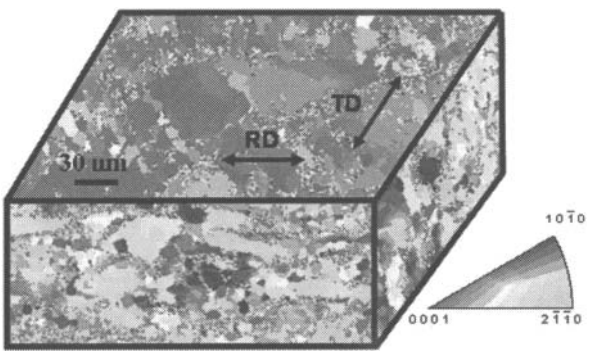

Figure 8. Schematic of the orientation texture of WE43-T5 in relation to the plate directions (not to scale).

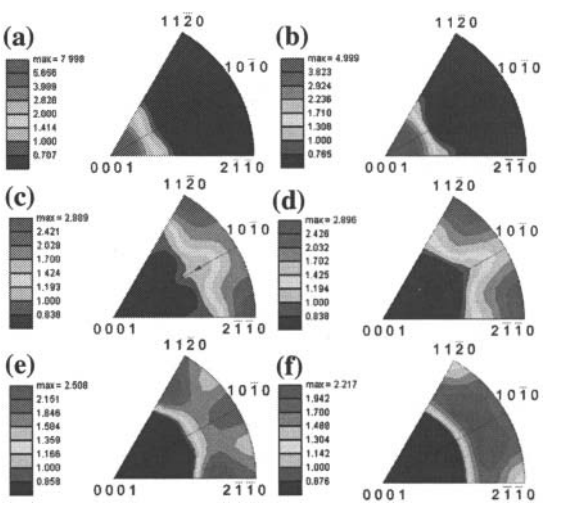

Figure 9. Inverse pole figures with texture index of (a) sample F surface parallel to the plane of the plate, (b) sample T5 surface parallel to the plane of the plate, (c) sample F surface perpendicular to the long transverse direction, (d) sample T5 surface perpendicular to the long transverse direction, (e) sample F surface perpendicular to the rolling direction, and (f) sample T5 surface perpendicular to the rolling direction.

Surface parallel to the plate had a higher amount of texturing than the surfaces perpendicular to the rolling and transverse directions. Although this is based on a limited dataset, Fig. 9 shows the homogenization and aging processes changes the orientation distribution, and decreases the texture.

Summary

The microstructure and tensile properties of Elektron™ WE43 –F and –T5 samples were characterized by microscopy techniques and in-situ tensile tests. Crystallographic orientation distribution results showed texturing of the surfaces, with the surface parallel to the plate surface having a basal plane orientation, and surfaces perpendicular to the rolling and transverse directions having a prismatic plane orientation. The in-situ tensile experiment results indicated a decrease in ductility but increase in the strength of the T5 alloys in both directions. The fracture surfaces suggest a change in the failure mechanism after the homogenization and artificial aging in the T5 alloys. More microstructural characterization and experiments are needed to determine the full effect of the homogenization and T5 tempering on the microstructure and the mechanics for future property optimization.

References

1. Magnesium Elektron, Elektron WE43 Wrought Alloy Datasheet: 478, www.magnesium-elektron.com

2. K. Cho, T. Sano, K. Doherty, C. Yen, G. Gazonas, J. Montgomery, and P. Moy, "Magnesium Technology and Manufacturing for Ultra Lightweight Armored Ground Vehicles," *Proceedings from the Army Science Conference* (2008).

3. M. Turski, J. F. Grandfield, T. Wilks, B. Davis, R. DeLorme, K. Cho, "Computer Modeling of DC Casting Magnesium Alloy WE43 Rolling Slabs," *Magnesium Technology 2010*, ed. S. R. Agnew, N. R. Neelameggham, E. A. Nyberg, and W. H. Sillekens (2010).

4. P. Mengucci, G. Barucca, G. Riontina, D. Lussana, M. Massazza, R. Ferragut, and E. Hassan Aly, "Structure Evolution of a WE43 Mg Alloy Submitted to Different Thermal Treatments," *Mater. Sci. Eng. A* 479 (2008) 37-44.

5. O. A. Lambri, W. Riehemann, L. M. Salvatierra, and J. A. Garcia, "Effects of Precipitation Processes on Damping and Elastic Modulus of WE 43 Magnesium Alloy," *Mater. Sci. Eng. A* 373 (2004) 146-157.

6. D. Lussana, M. Massazza, and G. Riontino, "A DSC Study of Precipitation Hardening in a WE43 Mg Alloy," *J. Thermal Analysis and Calorimetry* 92 (2008) 1, 223-225.

7. Z. Zhao, Q. Chen, Y. Wnag, and D. Shu, "Microstructures and Mechanical Properties of AZ91D Alloys with Y Addition," *Mater Sci. Eng. A* 515 (2009) 152-161.

8. J. F. Nie, "Effects of Precipitate Shape and Orientation on Dispersion Strengthening in Magnesium Alloys," *Scripta Mater.* 48 (2003) 1009-1015.

9. ARL report number ARL-TR-5212

10. J. Nie and B. C. Muddle, "Precipitation in Magnesium Alloy WE54 During Isothermal Ageing at 250 °C," *Scripta Mater.* 40 (1999) 1089-1094.

11. J. G. Wang, L. M. Hsiung, T. G. Nieh, and M. Mabuchi, "Creep of a Heat Treated Mg-4Y-3RE Alloy," *Mat. Sci. Eng. A* 315 (2001) 81-88.

12. F. Penghuai, P. Liming, J. Haiyan, Z. Zhenyan, Z. Chunquan, "Fracture Behavior and Mechanical Properties of Mg-4Y-2Nd-1Gd-0.4Zr (wt%) Alloy," *Mater Sci. Eng. A* 486 (2008) 572-579.

13. F. Hnilica, V. Janík, B. Smola, I. Stulíková, and V. Očenášek, "Creep Behaviour of the Creep Resistant MgY3Nd2Zn1Mn1 Alloy," *Mater Sci. and Eng. A* 489 (2008) 93-98.

14. J. W. Senn and S. R. Agnew, "Texture Randomization of Magnesium Alloys Containing Rare Earth Elements," *Magnesium Technology 2008*, ed. M. O. Pekguleryuz, N. R. Neelameggham, R. S. Beals, and E. A. Nyberg (2008).